

Multistage Kondo effect as a manifestation of dynamical symmetries in the single- and two-electron tunneling

K. Kikoin

*Raymond and Beverly Sackler Faculty of Exact Sciences,
School of Physics and Astronomy, Tel-Aviv University, Tel-Aviv 69978 Israel*

The concept of dynamical symmetries is used for formulation of the renormalization group approach to the Kondo effect in the Anderson model with repulsive and attractive interaction U . It is shown that the generic local symmetry of the Anderson Hamiltonian is determined by the $SU(4)$ Lie group. The Anderson Hamiltonian is rewritten in terms of the Gell-Mann matrices of the 4-th rank, which form the set of group generators and the basis for construction of irreducible vector operators describing the excitation spectra in the charge and spin sectors. The multistage Kondo screening is described in terms of the local $SU(4)$ dynamical symmetry. It is shown that the similarity between the conventional Kondo cotunneling effect for spin 1/2 in the positive U model and the Kondo resonance for pair tunneling in the negative U model is a direct manifestation of implicit $SU(4)$ symmetry of the Anderson/Kondo model.

PACS numbers: 71.10.Ca, 71.38.Mx, 72.15.Qm, 73.23.Hk, 73.63.Kv, 74.55.+v, 85.35.Gv

I. INTRODUCTORY REMARKS

In the 60-es and 70-es, when the basic concepts of dynamical symmetries have been formulated and elaborated,¹⁻⁶ only few physical realizations of these symmetries could be found in the realm of existing quantum mechanical objects (see^{7,8} for a review). One may mention the hydrogen atom⁹⁻¹¹ and the harmonic oscillator in various spatial dimensions¹²⁻¹⁴ as the systems for which the study of their dynamical symmetries revealed additional facets of excitation spectra and response to external fields. Rapid progress in the nanotechnology and nanophysics during two recent decades significantly extended the field of applicability of these concepts and enriched the theory with some new ideas.

Contemporary nanophysics¹⁵⁻¹⁹ deals with the artificial structures which consist of finite number of electrons confined within a tiny region of space, where the energy spectrum of electrons is discrete. As a result, such objects can be treated as "zero-dimensional" artificial atoms or molecules with spatially quantized discrete states, well defined symmetry and controllable electron occupation. Besides, modern technologies allow fabrication of devices where a "natural" atom or molecule is spatially isolated from the rest part of a device, so that the physical properties of an *individual* atom or atomic cluster may be studied experimentally.

In this paper we analyze the dynamical symmetries which arise when a group theoretical approach is used in the description of a contact between a few electron nanosystem \mathcal{S} with definite symmetry $G_{\mathcal{S}}$ and a macroscopic system \mathcal{B} ("bath" or "reservoir"). Due to this contact the symmetries of the system \mathcal{S} and the corresponding conservation laws are violated. If the contact between two systems is weak enough, the dynamics of interaction may be described in terms of transitions between the eigenstates of a system \mathcal{S} belonging to different irreducible representations of the group $G_{\mathcal{S}}$ generated by

the operators which obey the algebra $\mathfrak{g}_{\mathcal{S}}$. If the operators describing transitions between these eigenstates together with generators of the group $G_{\mathcal{S}}$ form the enveloping algebra $\mathfrak{d}_{\mathcal{S}}$ for the algebra $\mathfrak{g}_{\mathcal{S}}$, one may say that the system \mathcal{S} possesses a dynamical symmetry characterized by some group $D_{\mathcal{S}}$. The dynamical symmetry group technique offers mathematical tools for the unified approach to quantum objects, which allows one to consider not only the spectrum of a system \mathcal{S} , but also its response to external perturbation violating the symmetry $G_{\mathcal{S}}$ and various complex many-body effects characterizing the interaction between the system \mathcal{S} and its environment \mathcal{B} . In this paper we discuss a general algorithm of dynamical symmetry group approach to the few electron objects $\mathcal{B} + \mathcal{S}$ and its practical application to the single-electron tunneling in complex quantum dots and single molecule transistors. This tunneling is described in a framework of the Anderson model with repulsive and attractive interaction between the confined electrons.

II. HUBBARD OPERATORS GENERATING THE SPECTRUM OF NANOOBJECT

Following the definition used in Ref. 11, we define the dynamical symmetry group $D_{\mathcal{S}}$ as a Lie group of finite dimension characterized by the irreducible representations which act in the whole Hilbert space of eigenstates $|l\lambda\rangle$ of the Schroedinger equation

$$\hat{H}|l\lambda\rangle = E_l|l\lambda\rangle \quad (2.1)$$

describing the quantum system \mathcal{S} . Here l is the index of irreducible representation and λ enumerates the lines of this representation. The projection operators

$$X_{(l)}^{\lambda\mu} = |l\lambda\rangle\langle l\mu| \quad (2.2)$$

play the central part in the procedure of construction of irreducible representations l of the group of Schroedinger

equation \mathbf{G}_S . The basic property of these operators is given by the equation

$$X_{(l)}^{\lambda\mu}|l'\nu\rangle = \delta_{ll'}\delta_{\mu\nu}|l\lambda\rangle. \quad (2.3)$$

One may add to the set (2.2) the operators

$$X_{(l'l')}^{\lambda\mu} = |l\lambda\rangle\langle l'\mu| \quad (2.4)$$

which project the states belonging to different irreducible representations ($l \neq l'$) of the group \mathbf{G}_S one onto another. These operator may be also used for construction of the Lie algebras \mathbf{d}_S generating the spectrum of eigenstates of the Schroedinger equation and transitions between these states. Unifying the notations $|l\lambda\rangle = |\Lambda\rangle$, we obtain the commutation relations

$$[X^{\Lambda\Lambda'}, \hat{H}] = (E_{\Lambda'} - E_{\Lambda})\hat{H} \quad (2.5)$$

The right hand side of Eq. (2.5) turns into zero provided the states Λ and Λ' belong to the same irreducible representation of the group \mathbf{G}_S .

If a closed algebra \mathbf{d}_S exists for the set of operators (2.2), (2.4), then one may state that the system described by the Hamiltonian (2.1) possesses the dynamical symmetry \mathbf{D}_S . This algebra is conditioned by the norm

$$\sum_{\Lambda} X^{\Lambda\Lambda} = 1 \quad (2.6)$$

and by the commutation relations for the operators $X^{\Lambda_1\Lambda_2}$. In the general case these relations may be presented in the following form²¹

$$[X^{\Lambda_1\Lambda_2}, X^{\Lambda_3\Lambda_4}]_{\mp} = X^{\Lambda_1\Lambda_4}\delta_{\Lambda_2\Lambda_3} \mp X^{\Lambda_3\Lambda_3}\delta_{\Lambda_1\Lambda_4} \quad (2.7)$$

The ‘‘general case’’ implies that the Fock space includes the states which may belong to different charge sectors, i.e. changing the state Λ_1 for the state Λ_2 means changing the number of fermions $\mathcal{N}_{\Lambda_2} \rightarrow \mathcal{N}_{\Lambda_1}$ in the many-particle system. If both $\mathcal{N}_{\Lambda_1} - \mathcal{N}_{\Lambda_2}$ and $\mathcal{N}_{\Lambda_3} - \mathcal{N}_{\Lambda_4}$ are odd numbers (Fermi-type operators), the plus sign should be chosen in Eq. (2.7). If at least one of these differences is zero or even number (Bose-type operators), one should take the minus sign.

The operators $X^{\Lambda_1\Lambda_2}$ were exploited by J. Hubbard as a convenient tool for description of elementary excitations in strongly correlated electron systems (SCES). His seminal model of interacting electron motion in a narrow band, known now as the Hubbard model^{20–22} was the first microscopic model of SCES for which the conventional perturbative approach based on the Landau Fermi liquid hypothesis turned out to fail. Now the realm of SCES is really vast, and the most of artificial nanostructures in fact belong to this realm. In particular, complex quantum dots under strong Coulomb blockade are typical examples of short Hubbard chains or rings.

The Hubbard operators (2.4) obeying the commutation relation (2.5) provide a convenient tool for construction of

the algebras generating the dynamical symmetry groups of the Schroedinger operator ($\hat{H} - E$) or the resolvent operator $\hat{R} = (\hat{H} - E)^{-1}$. These operators may be used for construction of the generators of the appropriate group \mathbf{D}_S and irreducible tensor operators $\mathcal{O}^{(r)}$ (scalars, $r = 0$, vectors, $r = 1$, and tensors $r = 2, 3 \dots$) which transform along the representations of the group \mathbf{D}_S :

$$\mathcal{O}_{\varrho}^{(r)} = \sum_{\Lambda\Lambda'} \langle \Lambda | \mathcal{O}_{\varrho}^{(r)} | \Lambda' \rangle X^{\Lambda\Lambda'}. \quad (2.8)$$

Here the index ϱ stands for the components of irreducible tensor operator of the rank r . On the one hand, it is clear that the operators $X^{\Lambda\Lambda'}$ generate all the eigenstates of the Hamiltonian \hat{H} from any given initial state Λ' . The components of the operator $\mathcal{O}^{(r)}$ form their own closed algebra, which characterizes the dynamical symmetry group provided the Hamiltonian \hat{H} possesses such symmetry. Having in mind the application of this technique to the geometrically confined nanoobjects, we restrict ourself by the discrete eigenstates.

The Clebsch-Gordan expansion (2.8) is the basic equation which allows one to treat the dynamical symmetries of nanoobjects in a systematic way. The principal difference between the dynamical symmetries of SCES and those of integrable models is that in the latter case the spectrum of the object and its dynamical symmetries are known exactly, while in the former case as a rule only some part of excitation spectra (usually its lower part) may be found analytically and classified by symmetry. This means that one may judge about the dynamical symmetry of the spectrum only within the definite energy interval \mathcal{E} . Respectively, the characteristic energy scale may be different for different problems.

Our main subject in this paper is the Kondo effect in quantum dots.^{23,24} The hierarchy of the energy scales in this problem is well known.^{25,26} The Kondo effect arises as a result of orthogonality catastrophe in the Anderson model,²⁷ where the conduction electrons in the Fermi sea of metallic electrodes play part of the subsystem \mathcal{B} and the strongly correlated electrons in the quantum dot represent the subsystem \mathcal{S} . The largest energy scales in the Anderson model are the width of conduction band D in the subsystem \mathcal{B} and the energy of Coulomb blockade Q in the subsystem \mathcal{S} . The electrons confined in the nanoobject (quantum dot) are characterized by the ionization energy ϵ_i . Next in the hierarchy of energies are the tunneling amplitude V and the tunneling rate $\Gamma = \pi\rho_0V^2$ characterizing the process of electron tunneling through the potential barrier, which separates two subsystems. Here ρ_0 is the density of electron states at the Fermi level ϵ_F of the electron liquid in the leads. The Kondo effect arises in the single-electron tunneling regime under the restrictions of strong Coulomb blockade Q . In this regime the charge transport between the source and drain electrodes constituting the subsystem \mathcal{B} is realized as the electron cotunneling, where an electron from the source may tunnel into the dot \mathcal{S} only provided another electron leaves the dot for the drain. Cotunnel-

ing, which arises in the fourth order in V , is characterized by the energy J . Finally, the energy scale of Kondo effect $E_K \sim \sqrt{D\Gamma} \exp(-1/\rho_0 J)$ characterizes the crossover from the weak coupling regime $J \ll 1$ to the strong coupling, where J is enhanced due to the multiple creation of low-energy electron-hole pairs in the leads in the process of cotunneling. The Kondo energy also scales the excitations above the ground "Kondo-singlet" state.^{25,26} The hierarchy of all these energies is

$$D, U \gg \epsilon_i \gg V \gg \Gamma \gg J \gg E_K \quad (2.9)$$

An effective way to describe the crossover from the weak coupling to the strong coupling Kondo regime is the renormalization group (RG) approach.²⁸⁻³² In this method the renormalization of parameters ϵ_i, Γ, J in (2.9) in the course of reduction of the energy scale \mathcal{E} from high energies $\sim D, U$ to low energies still exceeding E_K is calculated. Our purpose is to describe this procedure in terms of dynamical symmetries *which change in the course of reduction of the energy scale \mathcal{E}* . It was noticed that the multistage Kondo screening predetermines the non-universal features of the Kondo tunneling in the quantum dots with even occupation.³³⁻³⁵ In that case the relevant dynamical symmetry groups are $SO(n)$ with $n = 4 - 8$.^{35,36} In this paper we will show that this language is useful already in the studies of the "ordinary" Kondo effect for quantum dots with odd electron occupation \mathcal{N} characterized by spin 1/2. The relevant Lie groups are $SU(n)$ with $n = 3, 4$.

III. DYNAMICAL SYMMETRIES IN QUANTUM DOTS

As was mentioned above, the dynamical symmetries of confined electrons in the quantum dot \mathcal{S} are revealed in its interaction with the "Fermi bath" \mathcal{B} of conduction electrons, The Anderson Hamiltonian describing the coupling between two subsystems reads

$$\hat{H} = \hat{H}_d + \hat{H}_b + \hat{H}_{db} \quad (3.1)$$

where three terms describe the nanoobject, the Fermi-bath and their coupling, respectively. The term \hat{H}_{db} in general case includes the direct coupling (quantum tunneling of electrons between two subsystems), the direct interaction of Coulomb and exchange nature and the indirect (kinematic) interaction induced by the tunneling. If the symmetry of nanoobject is well defined, the Hamiltonian \hat{H}_d may be diagonalized by means of projection operators (2.2), and the generators of dynamical symmetry group (2.8) arise in the interaction term \hat{H}_{db} in combination with the operators describing the excitations in the Fermi bath. These symmetries cannot be treated in the same way as the symmetries of the integrable systems discussed in the monographs 7,11 and the references therein, because the interaction not only activates the symmetry

$D_{\mathcal{S}}$ of the nanoobject but also involves the charge, orbital and spin degrees of freedom of the bath. This principal difference was pointed out in Refs. 35, where the quantum tunneling through an artificial molecule (double quantum dot) with even electron occupation $\mathcal{N} = 2$ in presence of the many-particle interaction of Kondo type was described by means of the generators of the $SO(4)$ group.

To take the dynamical symmetries explicitly in the calculations of excitation spectra and in the studies of spin and charge transport in nanoobject, one should adhere the following paradigm:³⁷

- When diagonalizing \hat{H}_d use the projection operators in accordance with Eqs. (2.1) – (2.5);
- Construct the operators $X^{\Lambda\Lambda'}$, which describe transitions between all the states in the "supermultiplet" of eigenstates of \hat{H}_d belonging both to the same and to different irreducible representations of the symmetry group $G_{\mathcal{S}}$ of the Hamiltonian \hat{H}_d and determine the relevant closed algebra generating the dynamical symmetry group $D_{\mathcal{S}}$;
- Rewrite \hat{H}_{db} in terms of the configuration change operators (2.4) belonging to adjacent charge sectors $\mathcal{N} \rightarrow \mathcal{N} \pm 1$;
- When projecting the original Anderson Hamiltonian (3.1) on the subspace of low-energy states $\langle \bar{\Lambda} | \dots | \bar{\Lambda} \rangle$ by means of the Schrieffer-Wolff (SW) transformation³⁸ or its generalizations, express the Hubbard operators which arise in this transformation via the generators of corresponding dynamical symmetry group using expansion (2.8).

To demonstrate this paradigm in action, let us consider the textbook example of a cell which may contain zero, one or two electrons with zero orbital moment. The Hamiltonian of this toy model

$$\hat{H}_d = \epsilon_d \sum_{\sigma=\uparrow,\downarrow} d_{i\sigma}^\dagger d_{i\sigma} + U n_{id\uparrow} n_{id\downarrow} \quad (3.2)$$

is nothing but the single-site Hamiltonian describing the elementary cell of the non-degenerate Hubbard model²⁰ with variable occupation number $\mathcal{N} = 0, 1, 2$ ("Hubbard atom"). Using definition (2.4) of the Hubbard operator, we rewrite \hat{H}_d in the universal form

$$\hat{H}_d = \sum_{\Lambda} E_{\Lambda} X^{\Lambda\Lambda} \quad (3.3)$$

where $\Lambda = 0, \sigma, 2$ and the energy levels E_{Λ} are

$$E_0 = 0, \quad E_{\uparrow} = E_{\downarrow} = E_1 \equiv \epsilon_d, \quad E_2 = 2\epsilon_d + U. \quad (3.4)$$

It is convenient to arrange the energy levels in accordance with the available charge and spin sectors (Fig. 1a). The arrows connecting the levels E_{Λ} and $E_{\Lambda'}$ correspond to the Hubbard operator $X^{\Lambda\Lambda'}$ and its complex

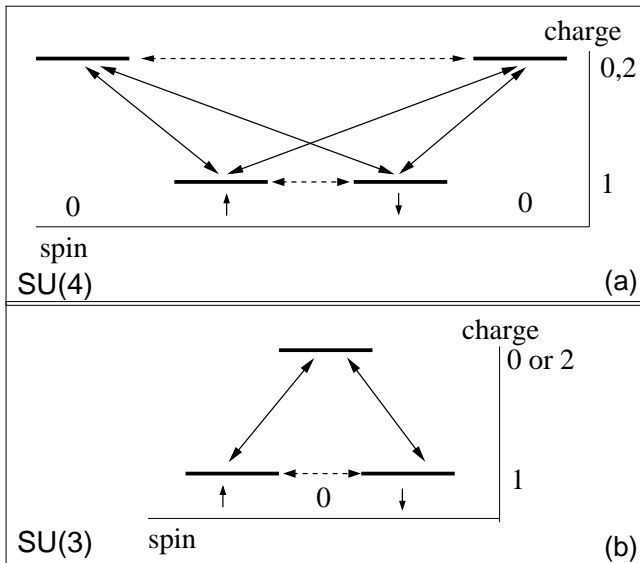


FIG. 1: (a): Scheme of the energy levels for a Hubbard atom with the $SU(4)$ dynamical symmetry describing transitions between the states with occupation $\mathcal{N} = 0, 1, 2$. (b) The same for a reduced spectrum with the $SU(3)$ dynamical symmetry describing transitions between the states with $\mathcal{N} = 0$ or 2 and $\mathcal{N} = 1$. The Bose-like transitions with even $\delta\mathcal{N} = 0, \pm 2$ are marked by the dashed arrows, the Fermi-like transitions with odd $\delta\mathcal{N} = \pm 1$ are marked by the solid arrows.

conjugate. This scheme visualizes the Fermi-like and Bose-like operators (solid and dashed lines, respectively), which obey the commutation relations (2.7). There are 15 such operators forming a closed superalgebra containing both commutators and anticommutators. The Hubbard operators may be regrouped into the generators of the $SU(4)$ group, known as the Gell-Mann matrices of 4th rank $\lambda_1 - \lambda_{15}$ (see Appendix). Thus the generic dynamical symmetry of Hubbard atom which is realized within the energy interval $\mathcal{E} \sim U, D$ is $SU(4)$.

Reduction of the energy scale to the interval $\epsilon_i < \mathcal{E} \ll U$ results in quenching the doubly occupied levels and corresponding reduction of the dynamical symmetry from $SU(4)$ to $SU(3)$ (Fig. 1b). The algebra generating this group contains eight Gell-Mann matrices of the 3rd rank $\lambda_1 - \lambda_8$ and the same number of Hubbard operators. Relations between the matrix of Hubbard operators and the Gell-Mann matrices for this group are also presented in Appendix. Further reduction of the energy interval $\mathcal{E} \ll \epsilon_i$ results in complete suppression of charged sectors $\mathcal{N} \neq 1$, so that we are left only with spin states $\sigma = \uparrow, \downarrow$. In this limit the dynamical symmetry is the same as the symmetry of the Hubbard atom, and the corresponding Lie group is $SU(2)$.

Mathematically, non-trivial dynamical symmetries are described by semisimple groups, possessing ideals. These ideals are formed by some triads of Gell-Mann matrices, e.g. matrices $\lambda_1, \lambda_2, \lambda_3$, which form a subgroup $SU(2)$ of a group $SU(n)$. If the states in the Fock space for the

Hubbard atom are ordered as

$$\bar{\Phi}_4 = (\uparrow \downarrow 0 2) \quad (3.5)$$

then the first three Gell-Mann matrices $\lambda_1 - \lambda_3$ are related to the spin states in the charge sector $\mathcal{N} = 1$ (see Appendix).

It is expedient to rewrite the original Hamiltonian (3.3) in terms of the generators of the group $SU(4)$ in the case where all four eigenstates (3.4) shown in Fig.1a are taken into account, and in terms of the $SU(3)$ generators in the case when the polar states with $\mathcal{N} = 2$ are frozen out (Fig.1b). In the full space $\bar{\Phi}_4$ we obtain by means of (A3)

$$\begin{aligned} \hat{H}_d^{SU(4)} &= \frac{E_0}{4} \left(1 - \frac{4}{\sqrt{3}} X_8 \right) \\ &+ \frac{E_1}{2} \left(1 + \frac{2}{\sqrt{3}} X_8 + \frac{2}{\sqrt{6}} X_{15} \right) \\ &+ \frac{h}{2} X_3 + \frac{E_2}{4} \left(1 - \sqrt{6} X_{15} \right) \end{aligned} \quad (3.6)$$

Here the notation X_ρ is used for the Gell-Mann matrices λ_ρ defined in the Fock space (3.5). The Zeeman term hS_z acting in the charge sector $\mathcal{N} = 1$ is also added. In the reduced Fock subspace

$$\bar{\Phi}_3 = (\uparrow \downarrow 0) \text{ or } (\uparrow \downarrow 2) \quad (3.7)$$

the Hamiltonian of the Hubbard atom rewritten with the use of Eqs. (A4) acquires quite compact form

$$\hat{H}_d^{SU(3)} = \frac{E_0}{3} \left(1 - \sqrt{3} X_8 \right) + \frac{E_1}{3} \left(1 + \sqrt{3} X_8 \right) + \frac{h}{2} X_3. \quad (3.8)$$

The Hubbard atom is a minimal model which can be used for description of a quantum dot with variable occupation \mathcal{N} coupled with the bath by means of the tunneling channel. The equilibrium occupation of the dot may be changed by means of injection of an electron or a hole from the metallic reservoir.¹⁵ This occupation fluctuates dynamically due to the single electron tunneling (SET) between the dot and the leads. The Coulomb blockade parameter Q plays the same part as the Coulomb repulsion U in the original Hubbard model. In the general case of, say, planar quantum dot the energy spectrum of a quantum dot contains many discrete states without definite angular symmetry. Only the highest occupied (HO) and the lowest unoccupied (LU) states are involved in single electron tunneling through such quantum dot. The Hamiltonian of subsystem \mathcal{S} in the Hamiltonian (3.1) has the form

$$\hat{H}_d = \sum_j \varepsilon_j d_{j\sigma}^\dagger d_{j\sigma} + \hat{H}_{\text{int}} + Q \left(n_{\text{dot}} - \frac{v_g C_g}{e} \right)^2 \quad (3.9)$$

Here the index j enumerates the levels bottom-up. \hat{H}_{int} is the electron-electron interaction in the quantum dot, Usually the self-consistent Hartree term is included in the

definition of discrete levels ε_j , and the relevant contribution to \hat{H}_{int} is the exchange between the electrons occupying different levels of a *neutral* quantum dot. $Q = e^2/2C$ is the capacitive energy of the dot, $n_{\text{dot}} = \sum_{j\sigma}^{(\text{ext})} d_{j\sigma}^\dagger d_{j\sigma}$ is the number of *extra* electrons or holes which are injected in the dot due to tunneling described by the Hamiltonian \hat{H}_{db} .

$$\hat{H}_{db} = \sum_{l=s,d} \sum_{jk\sigma} \left(W_{lj} d_{j\sigma}^\dagger c_{lk\sigma} + \text{H.c.} \right). \quad (3.10)$$

Corrections to the capacitive energy take into account the capacitance of the gate C_g and the gate voltage v_g . If the hierarchy of the energy scales

$$Q > (\delta\varepsilon, J) \gg W_{lj} \quad (3.11)$$

takes place ($\delta\varepsilon$ is the interlevel spacing between the HO and LU states, J is the exchange coupling constant), then one may assert that the charge transfer through the quantum dot occurs in the SET regime.

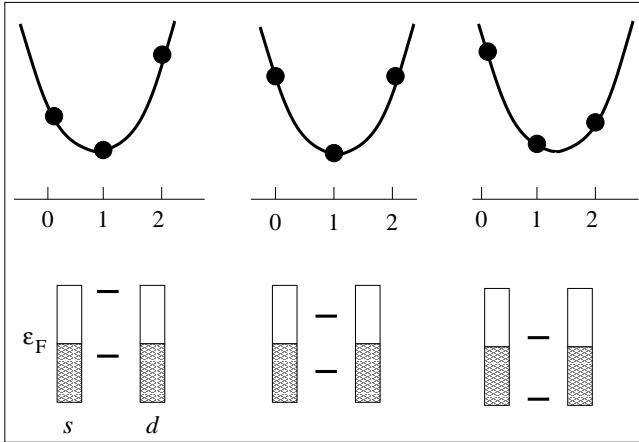


FIG. 2: Upper panel: Variation of the energy of the quantum dot $E_{\text{el}}(\mathcal{N})$ as a function of the gate voltage. Lower panel: corresponding variation of addition energies for electron and hole excitations relative to the Fermi level in the leads. See the text for further discussion.

Variation of the energy spectrum and the occupation of the quantum dot as a function of a gate voltage is exemplified in Fig. 2. The "Hubbard parabolas"²⁰⁻²² represent the energy $E_{\text{el}}(\mathcal{N})$ of the isolated quantum dot with the Hamiltonian (3.9). Three subsequent diagrams for the occupation $\mathcal{N} = 1$ show the asymmetric configurations with quenched zero and two electron occupation (the side diagrams) and the configuration with particle-hole symmetry (the middle diagram). The single particle excitations are the addition and extraction energies $E(\mathcal{N}) - E(\mathcal{N} \mp 1)$ which should be compared with the chemical potential of the bath (the Fermi energy) – see the lower panel of Fig. 2.

Following the above scheme, we express the Hubbard Hamiltonian (3.6) and the tunneling term H_{db}

$$H_{db} = \sum_{k\sigma} (t_k d_{k\sigma}^\dagger c_{k\sigma} + \text{H.c.}) \quad (3.12)$$

via the operators from the triads (A2) which are connected with the original Hubbard operators $X^{\Lambda\Lambda'}$ acting in the space (3.5) by the following relations:

$$\begin{aligned} \mathbb{T}^+ &= X^{\uparrow\downarrow}, & \mathbb{T}^- &= X^{\downarrow\uparrow}, & \mathbb{T}_z &= X^{\uparrow\uparrow} - X^{\downarrow\downarrow} \\ \mathbb{V}^+ &= X^{\uparrow 0}, & \mathbb{V}^- &= X^{0\uparrow}, & \mathbb{V}_z &= X^{\uparrow\uparrow} - X^{00} \\ \mathbb{U}^+ &= X^{\downarrow 0}, & \mathbb{U}^- &= X^{0\downarrow}, & \mathbb{U}_z &= X^{\downarrow\downarrow} - X^{00} \\ \mathbb{W}^+ &= X^{\uparrow 2}, & \mathbb{W}^- &= X^{2\uparrow}, & \mathbb{W}_z &= X^{\uparrow\uparrow} - X^{22} \\ \mathbb{Y}^+ &= X^{\downarrow 2}, & \mathbb{Y}^- &= X^{2\downarrow}, & \mathbb{Y}_z &= X^{\downarrow\downarrow} - X^{22} \\ \mathbb{Z}^+ &= X^{02}, & \mathbb{Z}^- &= X^{20}, & \mathbb{Z}_z &= X^{00} - X^{22} \end{aligned} \quad (3.13)$$

Equations (3.13) realize the general expansion scheme (2.8) for the irreducible *vector* operators in the group $SU(4)$. The triad $\vec{\mathbb{T}}$ is nothing but the set of spin 1/2 operators ($S^+, S^-, 2S_z$) acting in the charge sector $\mathcal{N} = 1$. The triad $\vec{\mathbb{Z}}$ describes the two-particle excitations ($\mathcal{N} = 0 \leftrightarrow \mathcal{N} = 2$). The rest four triads describe transitions between different charge sectors ($\mathcal{N} = 1 \leftrightarrow \mathcal{N} = 0, 2$). These operators enter the Anderson Hamiltonian corresponding to the Hubbard parabolas of Fig. 2.

The Hamiltonian $\hat{H}_d^{SU(n)}$ may be expressed via the z -components of irreducible vectors (3.13) by means of the following relations

$$\begin{aligned} \mathbb{P} &= \mathbb{V}_z + \mathbb{U}_z = X^{11} - 2X^{00}, \\ \mathbb{Q} &= \mathbb{W}_z + \mathbb{Y}_z = X^{11} - 2X^{22}, \\ \mathbb{R} &= \mathbb{P} - \mathbb{Q} = 2(X^{22} - X^{00}) \end{aligned} \quad (3.14)$$

and the completeness condition (2.6) which in this case reads

$$X^{00} + X^{11} + X^{22} = 1, \quad X^{11} = \sum_{\sigma} X^{\sigma\sigma} \quad (3.15)$$

[see also Eq. (A5)]. We find from Eqs. (3.14) and (3.15):

$$\begin{aligned} X^{00} &= \frac{1}{4} - \frac{1}{8}(3\mathbb{P} - \mathbb{Q}) \\ X^{22} &= \frac{1}{4} + \frac{1}{8}(\mathbb{P} - 3\mathbb{Q}) \\ X^{11} &= \frac{1}{2} + \frac{1}{4}(\mathbb{P} + \mathbb{Q}). \end{aligned} \quad (3.16)$$

Then the general $SU(4)$ configurations (the first and the third parabolas in Fig. 2) are described by the Hamiltonian

$$\begin{aligned} \hat{H}^{SU(4)} &= \frac{2E_1 + E_0 + E_2}{4} \cdot \mathbb{1} + \frac{h}{2} \cdot \mathbb{T}_z \\ &+ \frac{E_{10}}{4} \cdot \mathbb{P} + \frac{E_{12}}{4} \cdot \mathbb{Q} + \frac{E_{20}}{8} \cdot \mathbb{R} \end{aligned} \quad (3.17)$$

where $\mathbb{1}$ is the unit matrix in the Fock space $\bar{\Phi}_4$, $E_{ij} = E_i - E_j$ are the addition/extraction energies. Thus the operators $\mathbb{P}/4$, $\mathbb{Q}/4$, $\mathbb{R}/8$ and $\mathbb{T}_z/2$ describe all Fermi- and Bose-like excitations shown in Fig. 1a. In the degenerate case $E_0 = E_2 \equiv E_e$ (second parabola in Fig. 2) this Hamiltonian reduces to

$$\hat{H}_d^{SU(4)} = \frac{E_1 + E_p}{2} \cdot \mathbb{1} + \frac{h}{2} \cdot \mathbb{T}_z + \frac{E_{1e}}{4} \cdot (\mathbb{Q} + \mathbb{P}) \quad (3.18)$$

The tunneling term \hat{H}_{db} also may be expressed via the generators of $SU(4)$ group, namely via the ladder operators:

$$\hat{H}_{db}^{SU(4)} = \sum_k t_k (\mathbf{V}^\dagger + \mathbf{W}^\dagger) c_{k\uparrow} + (\mathbf{U}^\dagger - \mathbf{Y}^-) c_{k\downarrow} + \text{H.c.} \quad (3.19)$$

In the strongly asymmetric situations (the side configurations in Fig. 2, where the excitation E_{01} is soft, whereas the excitation E_{21} is frozen out or v.v.), the symmetry of the dot is reduced from $SU(4)$ to $SU(3)$. Respectively, the system (3.16) reduces to

$$X^{00} = \frac{1}{3} - \frac{\mathbf{P}}{3}, \quad X^{11} = \frac{2}{3} + \frac{\mathbf{P}}{3}, \quad (3.20)$$

or, in terms of operators \mathbf{U}, \mathbf{V}

$$X^{\uparrow\uparrow} = \frac{1}{3} + \frac{2\mathbf{V}_z - \mathbf{U}_z}{3}, \quad X^{\downarrow\downarrow} = \frac{1}{3} + \frac{2\mathbf{U}_z - \mathbf{V}_z}{3}. \quad (3.21)$$

The Anderson Hamiltonian acting in the space $\bar{\Phi}_3$ has the form

$$\hat{H}_d^{SU(3)} = \frac{2E_1 + E_0}{3} \cdot 1 + \frac{E_{10}}{3} \cdot (\mathbf{U}_z + \mathbf{V}_z) + \frac{\hbar}{2} \cdot \mathbf{T}_z \quad (3.22)$$

$$\hat{H}_{db}^{SU(3)} = \sum_k t_k [(\mathbf{V}^+ c_{k\uparrow} + \mathbf{U}^+ c_{k\downarrow}) + \text{H.c.}] \quad (3.23)$$

Thus the operators describing the charge Hubbard excitations in $SU(3)$ subspace $\bar{\Phi}_3$ (3.7) are $\bar{\mathbf{U}}, \bar{\mathbf{V}}$, whereas the spin excitations are described by the conventional spin operator $\bar{\mathbf{S}} = \bar{\mathbf{T}}/2$.

The dynamics of charge and spin excitations in this case is predetermined by the commutation relations for the group generators. The operators \mathbf{O} belonging to the same subgroup (triad) commute in accordance with the standard $SU(2)$ relations

$$[\mathbf{O}_z, \mathbf{O}^\pm] = \pm 2\mathbf{O}^\pm, \quad [\mathbf{O}^+, \mathbf{O}^-] = \mathbf{O}_z. \quad (3.24)$$

The non-zero commutation relations between the operators belonging to different triads ensure complex dynamical properties of Hubbard-like SCES.

$$\begin{aligned} [\mathbf{U}^\pm, \mathbf{V}^\mp] &= \pm \mathbf{T}^\mp, \quad [\mathbf{U}^\pm, \mathbf{V}_z] = \mp \mathbf{U}^\pm, \\ [\mathbf{U}_z, \mathbf{V}^\pm] &= \pm \mathbf{V}^\pm, \quad [\mathbf{U}_z, \mathbf{V}_z] = 0. \end{aligned} \quad (3.25)$$

Respectively, the non-zero anticommutation relations are

$$\begin{aligned} \{\mathbf{U}^+, \mathbf{U}^-\} &= \frac{2 + \mathbf{V}_z - 2\mathbf{U}_z}{3} \\ \{\mathbf{V}^+, \mathbf{V}^-\} &= \frac{2 + \mathbf{U}_z - 2\mathbf{V}_z}{3} \end{aligned} \quad (3.26)$$

Then the excitations in the charge sector are described by the Green functions, which may be found directly from equations of motion for the generators of $SU(3)$ group.

$$G_v = \langle\langle \mathbf{V}^-(t) \mathbf{V}^+(0) \rangle\rangle, \quad G_u = \langle\langle \mathbf{U}^-(t) \mathbf{U}^+(0) \rangle\rangle, \quad (3.27)$$

Respectively, the excitations in the spin sector are given by the Green functions

$$G_s = \langle\langle \mathbf{S}^-(t) \cdot \mathbf{S}^+(0) \rangle\rangle, \quad (3.28)$$

Here the double brackets stand for thermal averaging and time-ordering operations specified for the retarded, advanced or causal Green function. These functions can be easily found in the atomic limit where only the term $\hat{H}_d^{SU(3)}$ is retained. Solving equation of motion for the "Fermi-like" Green functions which describe excitations in the charge sector, one gets by means of the commutation and anticommutation relations (3.25) and (3.26):

$$\begin{aligned} G_v(\omega) &= \frac{i}{2\pi} \frac{(2 + \langle \mathbf{V}_z \rangle - 2\langle \mathbf{U}_z \rangle)/3}{\omega - \epsilon_d}, \\ G_u(\omega) &= \frac{i}{2\pi} \frac{(2 + \langle \mathbf{U}_z \rangle - 2\langle \mathbf{V}_z \rangle)/3}{\omega - \epsilon_d}. \end{aligned} \quad (3.29)$$

Using the definitions (3.20) and (3.21), we see that the numerators in the Green functions (3.29) are nothing but the averages $\langle X^{00} \rangle + \langle X^{\uparrow\uparrow} \rangle$ and $\langle X^{00} \rangle + \langle X^{\downarrow\downarrow} \rangle$, so that these functions are indeed the atomic Green functions for the Hubbard model²² rewritten in terms of the generators of the $SU(3)$ group.

The "Bose-like" Green function G_s which describes the excitations in the spin sector in the atomic limit has the usual form

$$G_s = \frac{i}{2\pi} \frac{\langle \mathbf{S}_z \rangle}{\omega - \hbar}. \quad (3.30)$$

A. Three-fold way for the Hubbard atom

As was noticed in the sixties,⁴ various families of hadrons are classified in accordance with the irreducible representations of $SU(3)$ group (see also Ref. 39). In particular, 18 baryons form two multiplets corresponding to representations $D^{(11)}$ (the octet of baryons with spin 1/2) and $D^{(30)}$ (the decuplet of baryons with spin 3/2). The octet of spinless mesons also transforms along the representation $D^{(11)}$. The higher representations of the $SU(3)$ group are realized in the physics of strong interaction because these "composite" particles possess not only the spin and charge but also the isospin and hypercharge quantum numbers, and the $SU(3)$ symmetry characterizes the latter variables. The elementary particles obeying the $SU(3)$ symmetry are the colored quarks. The $SU(3)$ symmetry in the hadron multiplets under strong interaction is satisfied only approximately due to existence of electro-weak interaction, so that this symmetry may be treated as a dynamical symmetry in the original sense of this notion.

The Hubbard atom with frozen doubly occupied states possesses only two quantum numbers, namely spin and charge. Therefore, the multiplet of Hubbard states is described by the lowest irreducible representation $D^{(10)}$ of the $SU(3)$ group. To construct this representation, one

should recollect that the two of eight Gell-Mann matrices can be diagonalized simultaneously. Following Ref. 39, we choose the representation with diagonal matrices T_z and Q . Then the set of allowed states is defined by two integer numbers λ, μ so that the eigenstates are determined as

$$M_T = \lambda + \mu, \quad M_Q = \frac{1}{3}(\lambda - \mu). \quad (3.31)$$

The whole set of eigenstates form a two-dimensional triangular lattice on the plane (M_T, M_Q) . Each irreducible representation $D^{\bar{\lambda}\bar{\mu}}$ is marked by the indices $\bar{\lambda}, \bar{\mu}$ corresponding to the state with the maximum eigenvalue \bar{M}_Q and the maximum value of \bar{M}_T possible at this \bar{M}_Q . Then the rest states forming this irreducible representation are constructed by means of the ladder operators T^\pm, U^\pm, V^\pm acting on the state $|\bar{M}_Q, \bar{M}_T\rangle$.

This procedure results in construction of the stars of basis vectors $\vec{D}^{\lambda\mu}$ and the polygons connecting the points generated by the ladder operators subsequently acting on the point (\bar{M}_Q, \bar{M}_T) . In the case of baryon family the corresponding multiplets are the hexagon with doubly degenerate central point for representation $D^{(11)}$ and the triangle with ten point in its vertices and on its sides for representation $D^{(30)}$. In the case of Hubbard atom the multiplet is represented by a triangle (Fig. 3) labeled in accordance with the state with the highest quantum numbers $\lambda = 1, \mu = 0$, which corresponds to the state $|\mathcal{N}, \sigma\rangle = |1, \uparrow\rangle$ of the Hubbard atom. Two remain-

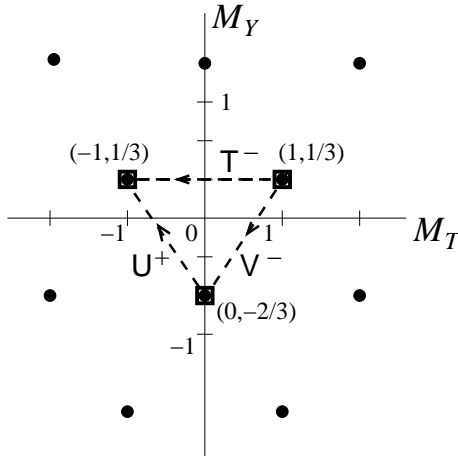


FIG. 3: Irreducible representation $D^{(10)}$ for the set $\bar{\Phi}_3$

ing components of the multiplet $\bar{\Phi}_3$ may be generated from the state $|1, \uparrow\rangle$ by means of the ladder operators $T^- = X^{\downarrow\uparrow}$ and $V^- = X^{0\uparrow}$. First of these operators corresponds to the "Bose-like" excitation with spin 1, and the second one is the "Fermi-like" excitation with spin 1/2. The triangle $D^{(10)}$ is closed by means of the operator $U^+ = X^{\downarrow 0}$. The interrelations between the values of the parameters λ, μ , the eigenvalues of the operators T_z and Q , and the eigenvalues $|\Lambda\rangle$ of the Hubbard Hamiltonian

are presented in the following table

λ	μ	M_T	M_Q	Λ
1	0	1	1/3	u
0	-1	-1	1/3	d
-1	1	0	-2/3	h

(3.32)

Here the notations u, d, h are used for the spin up, spin down and hole states, respectively.

Thus we see that the dual nature of the Hubbard operators manifested in the superalgebra with the commutation relations (2.7) allows one to use them for construction of the generic $su(3)$ algebra formed by the spin and pseudospin operators with the commutation relations (3.24), (3.25).

Like in the case of baryons and mesons, this symmetry is violated due to interaction with other subsystems. In our case this is the Fermi bath \mathcal{B} . The source of this interaction is the tunneling coupling given by the Hamiltonian $\hat{H}_{db}^{SU(3)}$. In analogy with the term offered by Gell-Mann and Ne'eman for the multiplet of light hadrons one may use the term "three-fold" (ternary) way for the SCES with approximate $SU(3)$ symmetry. Generalization of this description for the $SU(4)$ group is straightforward. In this case the phase space for the irreducible representations is defined by the eigenvalues of the operators P, Q, T_z , and the lowest irreducible representation of this group $D^{(100)}$ is represented by a triangular pyramid in this 3D space.

In the next section we will see how the hierarchy of dynamical symmetries of the Hubbard atom manifests itself in the RG evolution of the Anderson-Kondo problem.

IV. TWO-STAGE RENORMALIZATION GROUP FOR $SU(3)$ AND $SU(4)$ ANDERSON HAMILTONIAN

The RG method is based on the idea of renormalization of model parameters, which are relevant at low energy as a result of the change of the scale of high energy excitations.³⁰ If the model is renormalizable, any such parameter $P(\varepsilon)$ may be represented as

$$P(\varepsilon) - P[(1 + \kappa)\varepsilon] = -\kappa\varepsilon P'(\varepsilon) \quad (4.1)$$

where κ is positive infinitesimal and the prime stands for the derivative. The quantity $-\kappa\varepsilon P'(\varepsilon)$ is the contribution to $P(\varepsilon)$ from the high-energy states which are to be integrated out, preserving the form of $P(\varepsilon)$ but changing its scale. Adopting this approach, we immediately notice the inevitability of the three- or two-stage RG procedure as a direct consequence of several energy scales inherent in the Anderson model and the dynamical $SU(n)$ symmetry of its excitation spectrum with $n = 4$ or 3.

Taking as an example the first of three Hubbard parabolas in Fig. 2, we see that in this case the highest energy scale is the addition energy $\mathcal{E} \sim \varepsilon_d + Q - \varepsilon_F$.

The corresponding generators of $SU(4)$ group are \vec{W}, \vec{Y} . The next energy scale $\mathcal{E} \sim \varepsilon_F - \epsilon_d$ is the extraction energy, and the relevant generators are \vec{U}, \vec{V} . The lowest energy scale $\mathcal{E} \ll t^2/\epsilon_d$ is introduced by the second-order cotunneling processes from the dot to the leads, which are accompanied by the spin flips in the dot and creation of the low-energy electron-hole pairs in the leads. The vector operator \vec{T} is responsible for these processes. In other words, we arrive to the the renowned Jefferson-Haldane-Anderson renormalization group (RG) procedure.^{31,32} Basing on the symmetry analysis of preceding section, the RG procedure may be described in terms of the generators of $SU(4)$ group and its subgroups with reduction of the symmetry $SU(4) \rightarrow SU(3) \rightarrow SU(2)$ following the reduction of the energy scale \mathcal{E} .

Let us rederive for example the scaling equations for the two stage RG $SU(3) \rightarrow SU(2)$ realized in the limit $U \rightarrow \infty$ in these new terms. In the Anderson model the change of the energy scale in Eq. (4.1) means the contraction of the electron bandwidth $D \rightarrow D - \delta D$ in \hat{H}_b . The renormalized quantities are the self energies $\Sigma_\eta(\varepsilon)$ of the Green functions (3.27) and (3.28), $\eta = u, v, s$. The tunneling Hamiltonian (3.23) gives the second-order self-energy part for the Green functions G_v, G_u (3.29)

$$\epsilon_d = E_{10} + \frac{\Gamma}{\pi} \int_0^D \frac{d\varepsilon}{E_{10} - \varepsilon} \quad (4.2)$$

where

$$\Gamma = \Gamma_u = \Gamma_v = \pi \sum_k |t_k|^2 \delta(\varepsilon_F - \varepsilon_k)$$

is the spin-independent tunneling rate. The transformation (4.1) results in the Jefferson-Haldane scaling equation^{31,32}

$$\frac{d\epsilon_d}{dD} = \frac{\Gamma}{\pi D} \quad (4.3)$$

with the scaling invariant

$$\epsilon_d^* = \epsilon_d + \frac{\Gamma}{\pi} \ln \left(\frac{\pi D}{\Gamma} \right). \quad (4.4)$$

Thus, the evolution of the resonance level is determined by the vectors \vec{U}, \vec{V} operating in the charge subsectors of the group $SU(3)$. The same second-order processes generate the four-tail vertices $\sim \mathbf{V}^+ \mathbf{U}^- c_{k\downarrow}^\dagger c_{k'\uparrow}, \mathbf{U}^+ \mathbf{V}^- c_{k\uparrow}^\dagger c_{k'\downarrow}$ etc. Using the commutation relations (3.25), these vertices are combined in the conventional Schrieffer-Wolff exchange interaction

$$H_{\text{SW}} = J \vec{S} \cdot \vec{s} \quad (4.5)$$

where $\vec{s} = N^{-1} \sum_{kk'} c_{k'\sigma}^\dagger \hat{\tau} c_{k'\sigma'}$ is the local spin operator for conduction electrons, $\hat{\tau}$ is the the vector of Pauli matrices $J \sim t_{k_F}^2/E_{10}$ is the indirect Kondo exchange. The scaling equations for this Hamiltonian may be derived by means of the Anderson's RG procedure.

In the symmetric configuration (middle parabola in Fig. 2) the Jefferson – Haldane – Anderson scaling theory is in fact the manifestation of reduction of the dynamical symmetry $SU(4) \rightarrow SU(2)$, in which the charge excitations represented by the vectors $(\vec{W}, \vec{Y}, \vec{U}, \vec{V})$ are frozen out in the process of renormalization and the subgroup \vec{T} describing the spin degrees of freedom in the charge sector $\mathcal{N} = 1$ represents the low-energy part of the spectrum responsible for the Kondo singularities. Five vectors of six triads available in the Gell-Mann set are involved in this two-stage procedure.

Another choice of 15 linearly independent generators of the $SU(4)$ dynamical symmetry is possible in the case where instead of the spin degeneracy of the ground state with $\mathcal{N} = 1$ the charge degeneracy of the two singlets with $\mathcal{N} = 0, 2$ is realized. Such a possibility arises in the negative U Anderson model.^{40–42} In this configuration the vector \vec{T} is excluded from the renormalization procedure due to quenching of the sector $\mathcal{N} = 1$ at low energies. Instead the vector \vec{Z} is involved in formation of the Kondo singularities. The attractive interaction between the electrons in the nanoobject in this model stems from the strong electron-phonon interaction. Starting with the Anderson – Holstein model where the phonon subsystem is represented by the single Einstein mode with the energy Ω_0 , one may perform the canonical transformation,⁴³ which transforms the electron-phonon interaction into the polaron dressing exponent for the electron tunneling rate, the polaron shift of discrete electron levels and the phonon mediated electron-electron interaction. The latter renormalizes the Hubbard interaction term in the Anderson Hamiltonian

$$U' = U - 2\lambda^2 \Omega_0. \quad (4.6)$$

Here λ is the electron-phonon coupling constant. In the limit of strong electron-phonon coupling the energy gain due to the phonon mediated interaction overcomes the energy loss due to the Hubbard repulsion, and one comes to the case $U' < 0$. The negative U model may be realized in the single electron molecular transistors.^{44–49} The interaction (4.6) should be included in the term \hat{H}_d , so that in the negative U case the Hubbard parabolas for the energy spectrum are reversed relative to the usual shape shown in the middle configuration of Fig. 2. The “turned over” diagrams corresponding to the two nearly symmetric configurations shown in Fig. 4. Like in the positive U case, the transitions between the levels in the Hubbard supermultiplet are described by the operators (3.13) generating the $SU(4)$ dynamical symmetry group. We consider here the configurations, where the singlet states $|\Lambda\rangle = |0\rangle, |2\rangle$ are degenerate or nearly degenerate, and the spin doublet $|\Lambda\rangle = |\uparrow\rangle, |\downarrow\rangle$ is an excited virtual state in the cotunneling processes. The two configurations presented in Fig. 4 correspond to the empty and completely filled two-electron shell of the Hubbard atom. They are connected by the particle-hole symmetry transformation, so it is enough to discuss one of them.

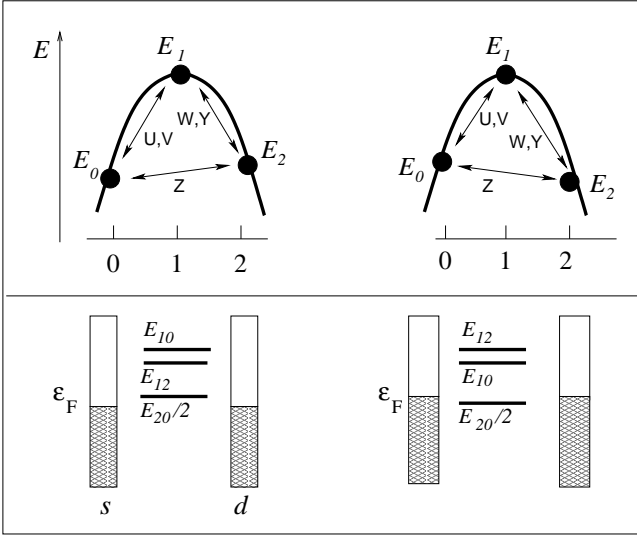


FIG. 4: Upper panel: inverted Hubbard parabolas for the negative U Hubbard atom in the cases of empty and doubly occupied shells. The interlevel transitions are described by the operators generating the $SU(4)$ dynamical group. Lower panel: single-electron levels corresponding to the transitions shown by the arrows in the upper panel (see the text for further explanation).

We will show below that the negative U Anderson model may be formally mapped on the positive U model, by means of the multistage RG method, which generalizes the Jefferson – Haldane – Anderson procedure^{28,31,32} mentioned above. In the positive U case after freezing out the high-energy excitations E_{01} and E_{21} corresponding to injection of a hole or of an electron into the singly occupied quantum dot at the Jefferson-Haldane stage of the renormalization, one arrives at the Anderson stage of Kondo screening of spin excitations in the sector $\mathcal{N} = 1$ described by the vector operator \vec{T} . In the negative U model the spin excitations are exponentially suppressed from the very beginning. After freezing out the charge excitations E_{10} and E_{12} generated by the operators $\vec{U}, \vec{V}, \vec{W}, \vec{Y}$ we are left only with the two-particle charge excitations E_{20} generated by the operator \vec{Z} .

Since the Jefferson-Haldane stage of the RG procedure is realized exactly in the same way as in the positive U Anderson model, we concentrate on the second stage, where the $SU(4)$ dynamical symmetry group is reduced to its $SU(2)$ subgroup represented by the triad \vec{Z} . These operators act in the subspace $\bar{\Phi}_2 = (0, 2)$. The effective SW Hamiltonian in this subspace reads

$$\hat{H}_{\text{cotun}} = N \frac{J_{\perp}}{2} (Z^+ B^- + Z^- B^+) + N J_{\parallel} Z_z B_z, \quad (4.7)$$

where the components of the vector \vec{Z} are presented in the last line of the system (3.13)]. The components of the vector \vec{B} defined in the space of two-particle itinerant

excitations are

$$\begin{aligned} B^+ &= N^{-1} \sum_{kk'} c_{k\uparrow}^{\dagger} c_{k'\downarrow}^{\dagger}, & B^- &= N^{-1} \sum_{kk'} c_{k\downarrow} c_{k'\uparrow}, \\ B_z &= N^{-1} \sum_{kk'} \left(c_{k\uparrow}^{\dagger} c_{k'\uparrow} - c_{k\downarrow} c_{k'\downarrow} \right) \\ &= N^{-1} \sum_{kk'} \sum_{\sigma} c_{k\sigma}^{\dagger} c_{k'\sigma} - 1 \end{aligned} \quad (4.8)$$

These operators obey the $su(2)$ commutation relations

$$[B^+, B^-] = B_z, \quad [B_z, B^{\pm}] = \pm B^{\pm} \quad (4.9)$$

The transversal part of the Hamiltonian (4.7) describes the tunneling of singlet electron pairs between the leads and the molecule, whereas its longitudinal part stems from the band electron scattering on the charge fluctuations.

Thus the Hamiltonian of two-electron tunneling is formally mapped onto the anisotropic Kondo Hamiltonian^{41,42,44} (see Fig.5). The origin of this anisotropy is the polaron dressing of tunneling matrix elements.⁴⁴ This dressing is different for the two-electron cotunneling and the electron scattering coupling parameters in the Hamiltonian (4.7). In the strong electron-phonon coupling limit, $(\lambda/\Omega_0)^2 = S \gg 1$

$$\frac{J_{\perp}}{J_{\parallel}} = \langle 2|0 \rangle \sim e^{-2(\lambda/\Omega_0)^2}. \quad (4.10)$$

The eventual source of this anisotropy is the overlap between the phonon wave functions for a molecule in the charge states $\mathcal{N} = 0$ and $\mathcal{N} = 2$, i.e. the Huang-Rhys factor S . In a framework of the Anderson RG scaling procedure this means that the renormalization diagrams for the two models are the same, namely the diagrams in the first and the second columns of Fig. 5 are mapped on the longitudinal and transversal components of the Kondo exchange Hamiltonian.(4.5) The mapping procedure implies the substitution $\vec{S} \rightarrow \vec{Z}$, $\vec{s} \rightarrow \vec{B}$. The scaling equations, which follow from these equations are the same as for the conventional anisotropic Kondo model,²⁸ namely

$$\frac{dj_{\parallel}}{d\eta} = -j_{\perp}^2, \quad \frac{dj_{\perp}}{d\eta} = -j_{\perp} j_{\parallel} \quad (4.11)$$

($j_i = \rho_0 J_i$). In the case of strong anisotropy (4.10) solution of this system gives for the Kondo temperature the following equation⁴⁴

$$T_K \sim \left(\frac{j_{\perp}}{j_{\parallel}} \right)^{1/j_{\parallel}} \sim \bar{D} \exp \left[-\frac{\pi \Omega_0}{2\Gamma} \left(\frac{\lambda}{\Omega_0} \right)^4 \right]. \quad (4.12)$$

The last equation in (4.12) is valid in the limit of strong electron-phonon coupling $S \gg 1$. Generally, the polaron narrowing of the tunneling rate results in a noticeable decrease of T_K in comparison with its value for the conventional Kondo effect.

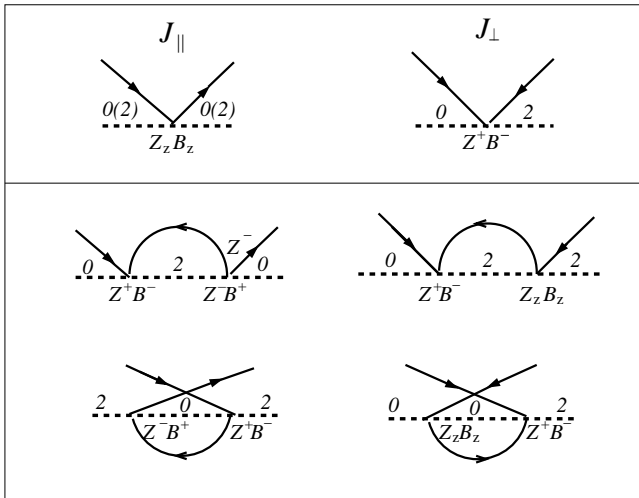


FIG. 5: RG diagrams in the space $\bar{\Phi}_2 = (0, 2)$. Upper panel: the bare vertices J_{\perp} for the two-electron tunneling and J_{\parallel} for the charge scattering. Lower panel: the diagrams for the second-order renormalization of these vertices. Solid lines stand for the conduction electron states, dashed lines denote the charge states of the molecule.

V. CONCLUDING REMARKS

In this paper we have shown that the “atomic” part \hat{H}_d of the Anderson Hamiltonian may be treated as a four-level system, so that the interlevel transitions induced by the tunneling term \hat{H}_{db} activate the implicit $SU(4)$ dynamical symmetry of the model. The symmetry is the same for the negative and positive U models. However, in spite of the formal similarity between the effective Hamiltonians for the single electron cotunneling and the electron pair cotunneling, the background physics is different in two versions of the Anderson model. In the positive U Anderson model the tunneling in the middle of the Coulomb window arises exclusively due to the many-body Abrikosov – Suhl resonance. In the negative U model the resonance conditions for the two-electron tunneling

arise at $E_{02} = 0$ irrelative to the many body particle-hole screening mechanism, so that the zero bias anomaly in the tunneling conductance exists already at $T \gg T_K$, as well as the finite bias anomaly at $E_{02} \neq 0$.^{47–49} One may say that the Anderson orthogonality catastrophe²⁷ responsible for the many-body Kondo-like screening at low T only enhances the two-electron tunneling resonance already sharpened due to non-orthogonality of the phonon clouds measured by the Huang – Rhys factor (4.10). The finite difference $E_{02} \neq 0$ in the negative U model is equivalent to the finite magnetic field in the positive U model: it results in the appearance of two split finite bias peaks in the tunneling conductance.

Having in mind all these differences, one may state that the multistage RG procedure reveals the hierarchy of reduced dynamical symmetries $SU(4) \rightarrow SU(3) \rightarrow SU(2)$ in the Anderson model both with the Hubbard repulsion for odd occupation and with the Hubbard attraction for even occupation and with the Hubbard repulsion for odd occupation and with the Hubbard attraction for even occupation. In this paper we confined ourselves with rephrasing the results already known in the Kondo physics, but we believe that the use of operators generating the set of the eigenstates of the zero Hamiltonian in the Anderson and Hubbard models and thus revealing its internal symmetry may facilitate the description of various dynamical properties of strongly correlated electron systems. In particular, new bosonization and fermionization procedures for the generators (3.13) alternative to the standard representations for the $SU(n)$ groups^{51–54} may be elaborated. We will turn to these procedures in the forthcoming publications.

Appendix A: GELL-MANN MATRICES AND HUBBARD OPERATORS

Here we summarize for the sake of convenience some properties of the Gell-Mann matrices of 4th rank and their realization in the Hubbard and Anderson models. The canonical form of these matrices describing the symmetry of four-level systems is

$$\begin{aligned}
\lambda_1 &= \begin{pmatrix} 0 & 1 & 0 & 0 \\ 1 & 0 & 0 & 0 \\ 0 & 0 & 0 & 0 \\ 0 & 0 & 0 & 0 \end{pmatrix}, \quad \lambda_2 = \begin{pmatrix} 0 & -i & 0 & 0 \\ i & 0 & 0 & 0 \\ 0 & 0 & 0 & 0 \\ 0 & 0 & 0 & 0 \end{pmatrix}, \quad \lambda_3 = \begin{pmatrix} 1 & 0 & 0 & 0 \\ 0 & -1 & 0 & 0 \\ 0 & 0 & 0 & 0 \\ 0 & 0 & 0 & 0 \end{pmatrix}, \\
\lambda_4 &= \begin{pmatrix} 0 & 0 & 1 & 0 \\ 0 & 0 & 0 & 0 \\ 1 & 0 & 0 & 0 \\ 0 & 0 & 0 & 0 \end{pmatrix}, \quad \lambda_5 = \begin{pmatrix} 0 & 0 & -i & 0 \\ 0 & 0 & 0 & 0 \\ i & 0 & 0 & 0 \\ 0 & 0 & 0 & 0 \end{pmatrix}, \quad \lambda_6 = \begin{pmatrix} 0 & 0 & 0 & 0 \\ 0 & 0 & 1 & 0 \\ 0 & 1 & 0 & 0 \\ 0 & 0 & 0 & 0 \end{pmatrix}, \\
\lambda_7 &= \begin{pmatrix} 0 & 0 & 0 & 0 \\ 0 & 0 & -i & 0 \\ 0 & i & 0 & 0 \\ 0 & 0 & 0 & 0 \end{pmatrix}, \quad \lambda_8 = \frac{1}{\sqrt{3}} \begin{pmatrix} 1 & 0 & 0 & 0 \\ 0 & 1 & 0 & 0 \\ 0 & 0 & -2 & 0 \\ 0 & 0 & 0 & 0 \end{pmatrix}, \quad \lambda_9 = \begin{pmatrix} 0 & 0 & 0 & 1 \\ 0 & 0 & 0 & 0 \\ 0 & 0 & 0 & 0 \\ 1 & 0 & 0 & 0 \end{pmatrix}, \\
\lambda_{10} &= \begin{pmatrix} 0 & 0 & 0 & -i \\ 0 & 0 & 0 & 0 \\ 0 & 0 & 0 & 0 \\ i & 0 & 0 & 0 \end{pmatrix}, \quad \lambda_{11} = \begin{pmatrix} 0 & 0 & 0 & 0 \\ 0 & 0 & 0 & 1 \\ 0 & 0 & 0 & 0 \\ 0 & 1 & 0 & 0 \end{pmatrix}, \quad \lambda_{12} = \begin{pmatrix} 0 & 0 & 0 & 0 \\ 0 & 0 & 0 & -i \\ 0 & 0 & 0 & 0 \\ 0 & i & 0 & 0 \end{pmatrix}, \\
\lambda_{13} &= \begin{pmatrix} 0 & 0 & 0 & 0 \\ 0 & 0 & 0 & 0 \\ 0 & 0 & 0 & 1 \\ 0 & 0 & 1 & 0 \end{pmatrix}, \quad \lambda_{14} = \begin{pmatrix} 0 & 0 & 0 & 0 \\ 0 & 0 & 0 & 0 \\ 0 & 0 & 0 & -i \\ 0 & 0 & i & 0 \end{pmatrix}, \quad \lambda_{15} = \frac{1}{\sqrt{6}} \begin{pmatrix} 1 & 0 & 0 & 0 \\ 0 & 1 & 0 & 0 \\ 0 & 0 & 1 & 0 \\ 0 & 0 & 0 & -3 \end{pmatrix},
\end{aligned} \tag{A1}$$

(see, e.g.⁵⁰). First eight matrices contain the 3-rd rank Gell-Mann operators of the $SU(3)$ group as submatrices. The operators $\lambda_9 - \lambda_{15}$ generate transitions between the triplet and the fourth level.

One may construct a subgroup $SU(2)$ of the group $SU(n)$ for any 2D subspace of the effective Fock space. There are three such "triads" grouped in three vectors $\vec{T}, \vec{U}, \vec{V}$ for the group $SU(3)$ with the symmetry operations acting in the 3D space $\bar{\Phi}_3$ (cf. Ref. 39). Adding fourth dimension provides three more vectors $\vec{W}, \vec{Y}, \vec{Z}$ representing the generators of the group $SU(4)$ together with the first three vectors.

$$\begin{aligned}
\mathsf{T}^\pm &= \frac{1}{2}(\lambda_1 \pm i\lambda_2), \quad \mathsf{T}_z = \lambda_3 \\
\mathsf{U}^\pm &= \frac{1}{2}(\lambda_6 \pm i\lambda_7), \quad \mathsf{U}_z = \frac{1}{2}(-\lambda_3 + \sqrt{3}\lambda_8) \\
\mathsf{V}^\pm &= \frac{1}{2}(\lambda_4 \pm i\lambda_5), \quad \mathsf{V}_z = \frac{1}{2}(\lambda_3 + \sqrt{3}\lambda_8), \\
\mathsf{W}^\pm &= \frac{1}{2}(\lambda_9 \pm i\lambda_{10}), \quad \mathsf{W}_z = \frac{1}{2}\left(\lambda_3 + \frac{1}{\sqrt{3}}\lambda_8 + \frac{4}{\sqrt{6}}\lambda_{15}\right) \\
\mathsf{Y}^\pm &= \frac{1}{2}(\lambda_{11} \pm i\lambda_{12}), \quad \mathsf{Y}_z = \frac{1}{2}\left(-\lambda_3 + \frac{1}{\sqrt{3}}\lambda_8 + \frac{4}{\sqrt{6}}\lambda_{15}\right) \\
\mathsf{Z}^\pm &= \frac{1}{2}(\lambda_{13} \pm i\lambda_{14}), \quad \mathsf{Z}_z = \frac{1}{\sqrt{3}}\left(-\lambda_8 + \sqrt{2}\lambda_{15}\right). \tag{A2}
\end{aligned}$$

The original Hubbard operators $X^{\Lambda\Lambda'}$ are represented via the Gell-Mann matrices in the basis $\bar{\Phi}_4$ (3.5) in the

following way:

$$\begin{aligned}
X^{\uparrow 0} &= \frac{1}{2}(\lambda_4 + i\lambda_5), \quad X^{0\uparrow} = \frac{1}{2}(\lambda_4 - i\lambda_5), \\
X^{\downarrow 0} &= \frac{1}{2}(\lambda_6 + i\lambda_7), \quad X^{0\downarrow} = \frac{1}{2}(\lambda_6 - i\lambda_7)/2, \\
X^{2\uparrow} &= \frac{1}{2}(\lambda_9 - i\lambda_{10}), \quad X^{\uparrow 2} = \frac{1}{2}(\lambda_9 + i\lambda_{10}) \\
X^{2\downarrow} &= \frac{1}{2}(\lambda_{11} - i\lambda_{12}), \quad X^{\downarrow 2} = \frac{1}{2}(\lambda_{11} + i\lambda_{12}) \\
X^{\uparrow\downarrow} &= \frac{1}{2}(\lambda_1 + i\lambda_2), \quad X^{\downarrow\uparrow} = \frac{1}{2}(\lambda_1 - i\lambda_2) \\
X^{20} &= \frac{1}{2}(\lambda_{13} - i\lambda_{14}), \quad X^{02} = \frac{1}{2}(\lambda_{13} + i\lambda_{14}) \\
X^{\uparrow\uparrow} &= \frac{1}{4}\left(1 + 2\lambda_3 + \frac{2}{\sqrt{3}}\lambda_8 + \frac{2}{\sqrt{6}}\lambda_{15}\right), \\
X^{\downarrow\downarrow} &= \frac{1}{4}\left(1 - 2\lambda_3 + \frac{2}{\sqrt{3}}\lambda_8 + \frac{2}{\sqrt{6}}\lambda_{15}\right), \\
X^{00} &= \frac{1}{4}\left(1 - \frac{4}{\sqrt{3}}\lambda_8 + \frac{2}{\sqrt{6}}\lambda_{15}\right), \\
X^{22} &= \frac{1}{4}(1 - \sqrt{6}\lambda_{15}) \tag{A3}
\end{aligned}$$

The tree operators $\mathsf{T}^\pm, \mathsf{T}_z$ from the first triad in the set (A2) describe the spin-flip excitations in the homopolar subspace $\mathcal{N} = 1$ of the Hubbard atom. The three operators $\mathsf{Z}^\pm, \mathsf{Z}_z$ from the last triad may be used in the description of excitations in the two-particle sector $\mathcal{N} = \{0, 2\}$ of

the Hubbard and Anderson model. The operators forming the triads \vec{U} and \vec{V} intermix the states from the charge sectors $\mathcal{N} = 0$ and $\mathcal{N} = 1$, and the operators \vec{W} and \vec{Y} do the same for the sectors $\mathcal{N} = 2$, $\mathcal{N} = 1$.

In many physical applications the reduced Anderson and Hubbard Hamiltonians with $U \rightarrow \infty$ are exploited. In this limit the doubly occupied state $|2\rangle$ is completely suppressed. In the appropriately reduced Fock space $\bar{\Phi}_3$ (3.7) possessing the $SU(3)$ symmetry the system (A3) transforms into

$$\begin{aligned} X^{\uparrow 0} &= \frac{1}{2}(\lambda_4 + i\lambda_5), & X^{0\uparrow} &= \frac{1}{2}(\lambda_4 - i\lambda_5), \\ X^{\downarrow 0} &= \frac{1}{2}(\lambda_6 + i\lambda_7), & X^{0\downarrow} &= \frac{1}{2}(\lambda_6 - i\lambda_7)/2, \\ X^{\uparrow\downarrow} &= \frac{1}{2}(\lambda_1 + i\lambda_2), & X^{\downarrow\uparrow} &= \frac{1}{2}(\lambda_1 - i\lambda_2) \\ X^{\uparrow\uparrow} &= \frac{1}{2} \left(\frac{2}{3} + \lambda_3 + \frac{1}{\sqrt{3}}\lambda_8 \right), \\ X^{\downarrow\downarrow} &= \frac{1}{2} \left(\frac{2}{3} - \lambda_3 + \frac{1}{\sqrt{3}}\lambda_8 \right), \\ X^{00} &= \frac{1}{3} \left(1 - \sqrt{3}\lambda_8 \right). \end{aligned} \quad (\text{A4})$$

Within each triad the standard Pauli commutation relations (3.24) for the components are valid. The commutation relations between the operators from different subgroups are described by more complicated structure factors.³⁹ These relations in our case may be derived from the general commutation relations (2.7) for the Hubbard operators (see the main text).

Two matrices used in the irreducible representation of the $SU(3)$ group are

$$T_z = \begin{pmatrix} 1 & 0 & 0 \\ 0 & -1 & 0 \\ 0 & 0 & 0 \end{pmatrix}, \quad Q = \frac{1}{3} \begin{pmatrix} 1 & 0 & 0 \\ 0 & 1 & 0 \\ 0 & 0 & -2 \end{pmatrix} \quad (\text{A5})$$

Their eigenvalues are

$$M_T = 1, -1, 0; \quad M_Q = 1/3, 1/3, -2/3 \quad (\text{A6})$$

for the states $|\uparrow\rangle, |\downarrow\rangle, |0\rangle$, respectively.

-
- ¹ Y. Ne'eman, Nucl. Phys. **26**, 222 (1961)
² M. Gell-Mann, Phys. Lett. **8**, 214 (1964).
³ G. Zweig CERN Reports No. 8181/Th 8419, 8419/Th 8412 (1964).
⁴ M. Gell-Mann and Y. Ne'eman, *The Eightfold Way* (Westview Press 1964).
⁵ A.O. Barut, Phys. Rev. **135**, B839 (1964).
⁶ Y. Dothan, M. Gell-Mann, and Y. Ne'eman, Phys. Lett. **17**, 148 (1965).
⁷ M.J. Englefield, *Group Theory and the Coulomb Problem* (Wiley, New York 1972).
⁸ I.A. Malkin and V.I. Man'ko, *Dynamical Symmetries and Coherent States of Quantum Systems* (Nauka, Moscow 1979), in Russian.
⁹ N. Mukunda, L. O'Raifeartaigh, and E.C.G. Sudarshan, Phys. Rev. Lett. **15**, 1041 (1965).
¹⁰ E.C.G. Sudarshan, N. Mukunda, and L. O'Raifeartaigh, Phys. Lett. **19**, 322 (1965).
¹¹ I.A. Malkin and V.I. Man'ko, Sov. Phys. - JETP Letters. **2**, 146 (1965); Sov. J. Nucl. Phys. **3**, 267 (1966).
¹² S. Goshen and H.J. Lipkin, Annals Phys. **6**, 301, 310 (1959).
¹³ A.O. Barut, Phys. Rev. **139**, B1433 (1965).
¹⁴ R.C. Hwa and J. Nuyts, Phys. Rev. **145**, 1188 (1966).
¹⁵ L.P. Kouwenhoven, D.G. Austing, and S. Tarucha, Rep. Progr. Phys., **64**, 701 (2001).
¹⁶ P.H. Sachrajda and M. Ciorga, *Nano-spintronics with lateral quantum dots* (Kluwer, Boston 2003).
¹⁷ *Molecular electronics*, Lecture Notes in Physics, vol. 680 (Eds. G. Cuniberti, G. Fagas, and K. Richter K, Springer, Berlin 2005).
¹⁸ D. Natelson, *Handbook of Organic Electronics and Photonics*. (American Scientific Publishers, Valencia, CA 2006).
¹⁹ R. Hanson, L. P. Kouwenhoven, J. R. Petta, S. Tarucha, and L.M.K. Vandersypen, Rev. Mod. Phys. **79**, 1217 (2007)
²⁰ J. Hubbard, Proc. Roy. Soc. A **276**, 238 (1963).
²¹ J. Hubbard, Proc. Roy. Soc. A **277**, 237 (1964).
²² J. Hubbard, Proc. Roy. Soc. A **281**, 401 (1964).
²³ L.I. Glazman and M.E. Raikh, Sov. Phys.- JETP Lett. **47**, 452 (1988).
²⁴ T.K. Ng and P.A. Lee, Phys. Rev. Lett. **61**, 1768 (1988).
²⁵ A.M. Tsvelik and P.B. Wiegmann, Adv. Phys. **32**, 453 (1983).
²⁶ N. Andrei, F. Furuya, and J.H. Loewenstein, Rev. Mod. Phys. **55**, 331 (1983).
²⁷ P.W. Anderson, Phys. Rev. Lett. **18**, 1049 (1967).
²⁸ P.W. Anderson, J. Phys. C: Solid. State Phys. **3**, 2346 (1970).
²⁹ A.A. Abrikosov and A.B. Migdal, J. Low Temp. Phys. **3**, 519 (1970).
³⁰ M. Fowler and A. Zawadowski, Solid State Commun. **9**, 471 (1971).
³¹ J.H. Jefferson, J. Phys. C: Solid. State Phys. **10**, 3589 (1977).
³² F. D. M. Haldane, Phys. Rev. Lett. **40**, 416 (1978).
³³ D. Giuliano and A. Tagliacozzo, Phys. Rev. Lett. **84**, 4677 (2000); D. Giuliano, B. Jouault, and A. Tagliacozzo, Phys. Rev. **63**, 125318 (2000).
³⁴ M. Eto and Yu. Nazarov, Phys. Rev. Lett. **85**, 1306 (2000); Phys. Rev. B **64**, 085322 (2001).
³⁵ K. Kikoin and Y. Avishai, Phys. Rev. Lett. **86**, 2090 (2001); Phys. Rev. B **65**, 115329 (2002).
³⁶ T. Kuzmenko, K. Kikoin, and Y. Avishai, Phys. Rev. Lett. **89**, 156602 (2002); Phys. Rev. B **69**, 195109 (2004).
³⁷ K. Kikoin, Y. Avishai and M.N. Kiselev. *Dynamical symmetries in nanophysics*, in "Nanophysics, Nanoclusters and Nanodevices," (Nova Science Publishers, New York 2006) pp. 39-86.

- ³⁸ J.R. Schrieffer and P.A. Wolff, Phys. Rev. **149**, 491 (1966).
- ³⁹ J. Elliot and P. Dauber, *Symmetry in Physics*, Ch.11 (Macmillan, London, 1979).
- ⁴⁰ P.W. Anderson, Phys. Rev. Lett. **34**, 953 (1975).
- ⁴¹ H.-B. Schüttler and A.J. Fedro, Phys. Rev. B **38**, 9063 (1988).
- ⁴² A. Taraphder and P. Coleman, Phys. Rev. Lett. **66**, 2814 (1991).
- ⁴³ I.G. Lang and Yu. A. Firsov, Sov. Phys. JETP **16**, 1301 (1963).
- ⁴⁴ P.C. Cornaglia, D.R. Grempel, and H. Ness, Phys. Rev. B **71**, 075320 (2005).
- ⁴⁵ P.C. Cornaglia and D.R. Grempel, Phys. Rev. B **71**, 245326 (2005).
- ⁴⁶ A.S. Aleksandrov, A.M. Bratkovsky, and R.S. Williams, Phys. Rev. B **67**, 075301 (2003).
- ⁴⁷ J. Koch, M.E. Raikh, and F. von Oppen, Phys. Rev. Lett. **96**, 056803 (2006).
- ⁴⁸ J. Koch, E. Sela, Y. Oreg, and F. von Oppen, Phys. Rev. B **75**, 195402 (2007).
- ⁴⁹ M. Leijnse, M. R. Wegewijs, and M. H. Hettler, Phys. Rev. Lett. **103**, 156803 (2009).
- ⁵⁰ T. Tilma, M. Byrd, and E.C.G. Sudarshan. J. Phys. A: Math. Gen. **35**, 10445 (2002).
- ⁵¹ N. Read and D.M. Newns, J. Phys. C **16**, 3273 (1983).
- ⁵² P. Coleman, Phys. Rev. B **29**, 3035 (1984).
- ⁵³ I. Affleck and B. Marston, Phys. Rev. B **37**, 3774 (1988).
- ⁵⁴ M.N. Kiselev, H. Feldmann, and R. Oppermann, Eur. Phys. J. B **22**, 53 (2001).